Journal of Materials Chemistry A

PAPER

View Article Online
View Journal | View Issue

Cite this: J. Mater. Chem. A, 2015, 3, 5556

Aluminium-rich Beta zeolite-supported platinum nanoparticles for the low-temperature catalytic removal of toluene†

Chunyu Chen, Qinming Wu, Fang Chen, Ling Zhang, Shuxiang Pan, Chaoqun Bian, Xiaoming Zheng, Xiangju Meng* and Feng-Shou Xiao

Received 24th November 2014
Accepted 15th January 2015

DOI: 10.1039/c4ta06407k

www.rsc.org/MaterialsA

The removal of volatile organic compounds is an important aspect of sustainability and environmental protection. Catalytic oxidation is one of the most efficient routes to achieve this. The K^+ form of an aluminium-rich Beta zeolite-supported Pt nanoparticle (2.2 nm) [Pt/KBeta-seed-directed synthesis (SDS)] catalyst is very active for the low-temperature catalytic removal of toluene and results in full conversion at a much lower temperature than a conventional KBeta-supported Pt nanoparticle (Pt/KBeta-TEA) catalyst. The higher activity of the Pt/KBeta-SDS catalyst compared with the Pt/KBeta-TEA catalyst is related to the advantages of the higher K^+ content and fewer terminal silanol defects in the KBeta-SDS catalyst than in the KBeta-TEA catalyst. The higher K^+ content is helpful for the formation of more Pt^0 species, and both the higher K^+ content and the lower number of terminal silanol defects are favourable for the adsorption of toluene, as evidenced by XPS and the toluene-TPD profiles. More importantly, the Pt/KBeta-SDS catalyst shows very stable activities in the presence of H_2O and CO_2 in the feed gases. The combination of this extraordinary activity and excellent stability in the catalytic removal of toluene over the Pt/KBeta-SDS catalyst are important for future environment protection.

1. Introduction

Volatile organic compounds (VOCs), which are emitted from motor vehicles and industrial processes as well as from indoor compounds, are major air pollutants. VOCs such as toluene, formaldehyde and halogenated hydrocarbons are precursors of ozone and photochemical smog, which are harmful to human health.[1–4] The complete removal of VOCs has received much attention and catalytic oxidation has been identified as one of the most effective and economically feasible routes for VOCs abatement without the creation of further toxic by-products, especially for low concentrations of VOCs at low temperatures.[5–18]

Zeolite-supported noble metal nanoparticles have been proved to be superior catalysts for the removal of VOCs as a result of a combination of the advantages of the zeolites (large surface area, high adsorption capacity, acid–base properties and high stability) and the noble metals (high activity and stability).[19–32] For example, Becker and Forster[19,20] studied the oxidative decomposition of benzene and its methyl derivatives over NaY, CuY, PdHY and PdY zeolites; PdY was the most active catalyst. The FAU zeolite, ZrO_2 and hierarchical macro-mesoporous ZrO_2 impregnated with 0.5% Pd have been compared as catalysts for the total oxidation of toluene; the combination of Pd/FAU zeolite had a higher activity than Pd loaded onto conventional ZrO_2 and macro-mesoporous ZrO_2.[21–23] Other workers have found that Pt/HFAU and Pt/HBEA exhibited very good activities in the catalytic oxidation of *o*-xylene, methyl-isobutyl-ketone and dichloromethane.[24–28] In addition, we found that ZSM-5-supported Pt catalysts had a superior performance in the catalytic removal of toluene. In particular, it was shown that K^+-exchanged ZSM-5 exhibited a better performance than the H^+ and Na^+ forms of zeolites and that the K^+ content in ZSM-5 was positively correlated with the catalytic activity in the removal of VOCs.[31]

In general, the K^+ content of zeolites is dependent on the ion-exchange capacity, which is associated with the Al species in the zeolite framework. For conventional Beta zeolite (Beta-TEA) synthesized in the presence of tetraethylammonium cations (TEA^+), the Si : Al ratios are usually >12. However, the template-free and seed-directed synthesis (SDS) of Beta zeolite (Beta-SDS) shows that the Si : Al ratios in this zeolite may be as low as 4, which significantly increases the Al species in the Beta framework. This feature is favourable for the introduction of more K^+ into the Beta zeolite.[33–36] Beta-SDS has fewer terminal silanol defects than Beta-TEA,[33,36] which is favourable for the adsorption of the hydrophobic molecules of VOCs.

We report here the successful synthesis of an aluminium-rich Beta zeolite with a relatively high K^+ content and few

Key Lab of Applied Chemistry of Zhejiang Province and Department of Chemistry, Zhejiang University, Hangzhou 310007, China. E-mail: mengxj@zju.edu.cn

† Electronic supplementary information (ESI) available: Supplementary tables and figures. See DOI: 10.1039/c4ta06407k

terminal silanol defects (KBeta-SDS) compared with conventional Beta zeolite. The KBeta-SDS-supported Pt nanoparticles (Pt/KBeta-SDS) exhibited extraordinary catalytic activity. The Pt/KBeta-SDS also showed excellent catalytic stability, even in the presence of H_2O and CO_2 in the feed gases.

2. Experimental

2.1 Materials

$NaAlO_2$, NaOH, HCl, ethanol and toluene were purchased from Sinopharm Chemical Reagent. Fumed silica (SiO_2) was purchased from Shenyang Chemical Co. Beta seeds (Si : Al = 12.50) were purchased from Nankai University Catalyst Co. Tetraethylammonium hydroxide solution (2.0 M in H_2O) was supplied by BASF. $H_2PtCl_6 \cdot 6H_2O$, ethylene glycol and KCl were purchased from Aladdin. Polyvinylpyrrolidone (PVP, M_w = 29 000) was purchased from Sigma-Aldrich. All these chemicals were of analytical-reagent grade and were used without further purification.

2.2 Preparation

The template-free and SDS of Beta zeolite (Beta-SDS) was carried out in the presence of calcined Beta zeolite seeds.[34] In a typical run, 0.32 g of $NaAlO_2$ and 0.56 g of NaOH were dissolved in 6.8 mL of H_2O, followed by the addition of 2.0 g of fumed silica. After stirring for 12 h, 0.1 g of Beta zeolite seeds was introduced into the gel and stirred for 10 min. The resultant gel was transferred into an autoclave to crystallize at 120 °C for 90 h. The solid product was filtered, washed with water and dried at 80 °C in air for 12 h. For comparison, conventional Beta zeolite (Beta-TEA) was synthesized in the presence of TEA^+. In a typical run, 0.15 g of $NaAlO_2$ and 0.08 g of NaOH were dissolved in 6.3 mL of H_2O, followed by the addition of 9.7 mL of tetraethylammonium hydroxide solution. After stirring for 10 min, 2.4 g of fumed silica were introduced into the gel and the mixture was stirred for 12 h. The resultant gel was transferred into an autoclave to crystallize at 140 °C for 96 h. The solid product was centrifuged, washed with water, dried at 80 °C in air for 12 h and calcined at 550 °C for 5 h to remove the organic template. The K^+-exchanges of the Beta zeolite were performed with 1 M KCl solution. In a typical run, 1.0 g of Beta zeolite was added into 50 mL of KCl solution, followed by stirring at room temperature for 3 h. The solid product was filtered or centrifuged, washed with water and dried at 80 °C in air for 12 h. To decrease the Na^+ concentration in the samples, the ion-exchange procedures were repeated once more.

Pt nanoparticles were synthesized by a previously reported polyol reduction method.[37,38] In a typical run, a solution of NaOH (0.22 g, 20 mL) was added into an ethylene glycol solution of $H_2PtCl_6 \cdot 6H_2O$ (20 mL) and stirred at room temperature for 1 h; a transparent yellow suspension was obtained. After heating at 90 °C for 2 h with an N_2 flow passing through the reaction system, a transparent dark brown homogeneous colloidal solution of Pt nanoparticles was obtained without any precipitate. The Pt nanoparticles were precipitated by adding 0.3 M HCl (pH 3–4), collected by centrifugation and dispersed in ethanol containing 40 mg PVP.[39]

KBeta zeolite-supported Pt nanoparticle catalysts were prepared by loading Pt nanoparticles onto the KBeta zeolites. In a typical run, a measured amount of KBeta was added into 50 mL of ethanol containing an appropriate amount of Pt nanoparticles, followed by stirring at room temperature for 12 h. The solid product was finally obtained by filtration or centrifugation, washed with ethanol, dried at 80 °C in air for 12 h, calcined at 350 °C in air for 12 h and reduced at 300 °C in an H_2 flow for 2 h.[39] In this work, KBeta-SDS- and KBeta-TEA-supported Pt nanoparticle catalysts are denoted as Pt/KBeta-SDS and Pt/KBeta-TEA; these samples without reduction are denoted as Pt/KBeta-SDS-unreduced and Pt/KBeta-TEA-unreduced, respectively.

2.3 Characterization

X-ray diffraction (XRD) patterns were obtained using a RIGAKU Ultimate IV diffractometer with Cu Kα radiation. Nitrogen sorption isotherms at −196 °C were measured using Micromeritics ASAP 2020M and Finetec Finesorb-3020 systems. The surface area was calculated by using the Brunauer–Emmett–Teller (BET) method. The elemental composition of the zeolites and the Pt content in the catalysts were determined by inductively coupled plasma atomic emission spectrometry (ICP-AES) using a Perkin-Elmer plasma 8000 optical emission spectrometer. The X-ray photoelectron spectra (XPS) of the catalysts were recorded using a Thermo ESCALAB 250 instrument with Al Kα X-ray radiation for the X-ray source. The binding energies were calibrated against the C1s (285.0 eV) and Al2p (73.9 eV) peaks. Temperature-programmed desorptions of toluene (toluene-TPD) were performed on a Finetec Finesorb-3010 instrument equipped with a thermal conductivity detector. In a typical run, 10 mg of sample were pre-treated in a pure He flow (15 mL min^{-1}) at 200 °C for 0.5 h and then cooled down to 50 °C prior to the adsorption of toluene for 2 h. After saturation with toluene, the sample was flushed with pure He (15 mL min^{-1}) for 2 h at 50 °C. The desorption profiles of toluene-TPD were recorded online at a heating rate of 10 °C min^{-1}. Scanning electron microscopy (SEM) images were recorded on a Hitachi SU 1510 apparatus. Transmission electron microscopy (TEM) and electron diffraction (ED) experiments were performed at 100 kV on a Hitachi HT-7700 electron microscope. High-resolution TEM (HRTEM) images were obtained at 200 kV on a JEOL 2100F electron microscope.

2.4 Catalytic evaluation

Experiments for the catalytic removal of 1000 ppm toluene were performed at atmospheric pressure in a continuous-flow fixed-bed microreactor consisting of a quartz tube (6 mm i.d.) filled with the catalyst. A typical experiment was performed using a catalytic bed of 100 mg catalyst (0.45–0.90 mm size) with a total flow-rate of feed gases (79% N_2 + 21% O_2) of 100 mL min^{-1}, giving a space velocity (SV) of 60 000 mL g^{-1} h^{-1}. The relative humidity (RH) of the feed gases was determined by a high-accuracy thermo-hygrometer with a probe (WSB-2-H2,

Zhengzhou Boyang). The concentration of toluene in the tail gases was analysed using a gas chromatograph (Kexiao, GC1690) equipped with a flame ionization detector and a 19091N-113 INNOWAX capillary column (Agilent, 30 m × 0.32 mm × 0.25 μm i.d.). The concentration of the oxidative products (CO_2 and CO) in the tail gases was analysed with a gas chromatograph (Kexiao, GC1690) equipped with a thermal conductivity detector using a Carboxen packed column (JieDao, 2 m × 2 mm). The conversion of toluene was calculated from the difference in the inlet and outlet concentrations of toluene. The selectivity to CO_2 was calculated from the consumption of toluene and the outlet concentration of CO_2. The carbon balance reached 100 ± 5% in this work. The catalytic activities were determined by the values of T_5, T_{50} and T_{98}, which were defined as the temperatures at 5%, 50% and 98% of toluene conversion, respectively.

3. Results and discussion

3.1 Sample preparation and characterization

3.1.1 As-synthesized Beta-SDS and Beta-TEA zeolites. Fig. S1† shows the XRD patterns, N_2 sorption isotherms and SEM images of the as-synthesized Beta-SDS and Beta-TEA samples. The XRD patterns show that both samples had well-resolved characteristic peaks associated with the BEA structure. The N_2 sorption isotherms show that the as-synthesized Beta-SDS already had open micropores, whereas the as-synthesized Beta-TEA had no open micropores. The SEM images show that both samples had a similar morphology, with almost uniform crystals of about 100–160 nm.

3.1.2 Pt nanoparticles. The Pt nanoparticles in this research were synthesized by a polyol reduction method. Fig. 1 shows the TEM images and size distribution of the Pt nanoparticles; the Pt nanoparticles were 2.2 ± 0.4 nm in size. The ED pattern of the Pt nanoparticles corresponded to the (111), (200), (220), (311) and (222) planes of the face-centred cubic lattice.[40] The HRTEM image of the Pt nanoparticles in the samples clearly showed the lattice fringes with interplanar distances of 0.23 nm, corresponding to Pt(111) planes.[41]

3.1.3 KBeta zeolite-supported Pt nanoparticle catalysts. The KBeta zeolite-supported Pt nanoparticle catalysts were prepared by loading Pt nanoparticles onto the KBeta zeolites. Fig. S2A† shows the XRD patterns of the various KBeta-based samples, which exhibit well-resolved characteristic peaks associated with the BEA zeolite structure. Fig. S2B† shows the N_2 sorption isotherms of these samples and their textural parameters are summarized in Table S2.† These results indicate that both KBeta-SDS and KBeta-TEA retain their textures after loading with Pt nanoparticles.

Fig. 2 shows TEM images and the Pt nanoparticle size distributions of Pt/KBeta-SDS and Pt/KBeta-TEA, indicating that both catalysts have a similar Pt particle size, with a distribution of 2.2 ± 0.4 nm. These results suggest that the Pt nanoparticle size distribution is unchanged after the loading process. The HRTEM images of these catalysts (insets, Fig. 2A) also show a Pt lattice with a Pt(111) interlayer spacing of 0.23 nm.[42]

Table 1 gives the elemental composition of Pt/KBeta-SDS and Pt/KBeta-TEA, indicating that both samples have a similar Pt loading (about 1.1%), but different K^+ contents. The K^+ content of Pt/KBeta-SDS is almost three times that of Pt/KBeta-TEA.

Fig. S3† shows the Pt4f XPS spectra of various KBeta-based samples. After deconvolution, the ratios of Pt^0/Pt^{2+} in the various samples could be estimated (Table 2). The Pt^0/Pt^{2+} ratios of the Pt/KBeta-SDS samples were higher than those of the Pt/KBeta-TEA samples, confirming that a higher K^+ content is favourable for the formation of more Pt^0 species, which are regarded as catalytically active centres for the conversion of toluene into CO_2 and H_2O.[24,30,31] The effect of the K^+ ions on the formation of Pt^0 species is suggested by the interaction between the framework oxygen with the Pt nanoparticles (Pt–zeolite interaction), where the framework oxygen in the zeolite is strongly influenced by the presence of K^+ ions. This Pt–zeolite interaction has been reported previously.[43–47] For example, Treesukol *et al.* reported that an interaction took place by electron transfer from the framework oxygen to the Pt atom in

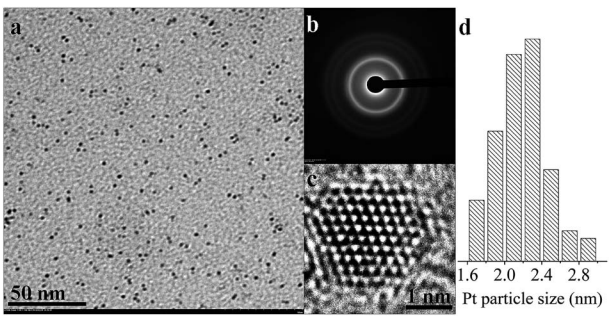

Fig. 1 (a) TEM image, (b) ED pattern, (c) HRTEM image and (d) size distribution of Pt nanoparticles.

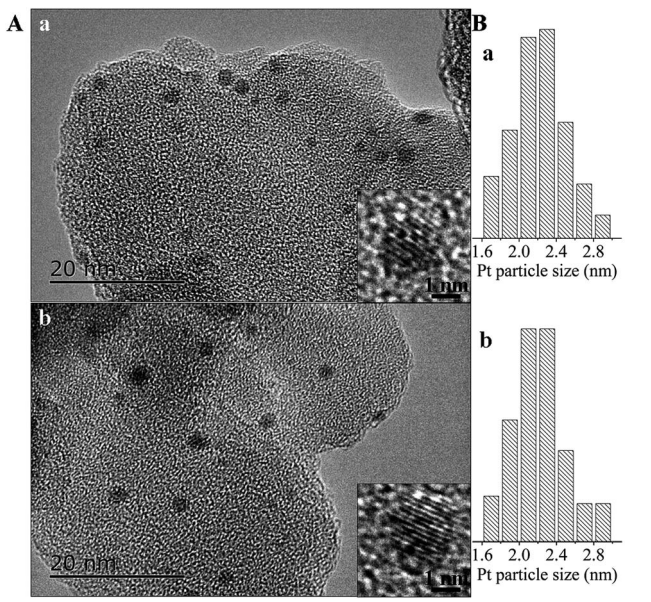

Fig. 2 (A) TEM images (inset, HRTEM images) and (B) Pt nanoparticle size distributions of (a) Pt/KBeta-SDS and (b) Pt/KBeta-TEA.

Table 1 Elemental composition of Pt/KBeta-SDS and Pt/KBeta-TEA

Sample[a]	Si : Al ratio	K (mg g^{-1})	Pt content (%)
Pt/KBeta-SDS	3.90	9.72	1.15
Pt/KBeta-TEA	10.66	3.30	1.07

[a] Determined from ICP-AES measurements.

Table 2 XPS results for the various samples

		Peak area		
Sample	Pt species	$Pt4f_{7/2}$	$Pt4f_{5/2}$	Pt^0/Pt^{2+a}
Pt/KBeta-SDS	Pt^0	781	588	3.9
	Pt^{2+}	202	152	
Pt/KBeta-SDS-unreduced	Pt^0	477	359	2.4
	Pt^{2+}	198	149	
Pt/KBeta-TEA	Pt^0	410	308	2.5
	Pt^{2+}	164	124	
Pt/KBeta-TEA-unreduced	Pt^0	385	289	1.8
	Pt^{2+}	209	157	

[a] Peak area ratio.

the Pt/ZSM-5 sample;[43] Koningsberger and coworkers showed that the metals at the interface may be sufficiently polarized to bond with the oxygen of supports such as zeolites.[44–46]

Fig. 3 shows the toluene-TPD profiles of Pt/KBeta-SDS and Pt/KBeta-TEA. Both samples gave three peaks, but Pt/KBeta-SDS showed much higher desorption temperatures (75, 160 and 345 °C) than Pt/KBeta-TEA (75, 148 and 275 °C), suggesting that Pt/KBeta-SDS adsorbs toluene more strongly than Pt/KBeta-TEA. This phenomenon could be reasonably assigned to the higher K^+ content and fewer terminal silanol defects in KBeta-SDS than in KBeta-TEA.[33–36,48,49] Yoshimoto *et al.*[48] comprehensively and quantitatively analysed the adsorption behaviour of toluene on alkaline-containing zeolites using a TPD method and reported that approximately one toluene molecule was adsorbed on one alkali cation in BEA and MFI zeolites at high temperatures.

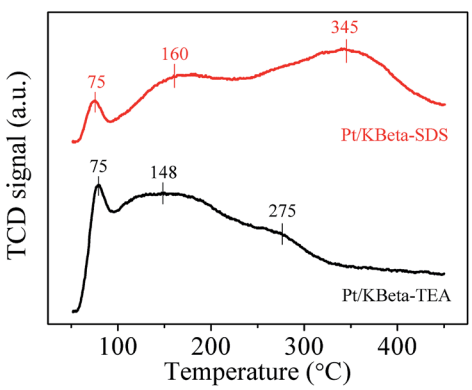

Fig. 3 Toluene-TPD profiles of Pt/KBeta-SDS and Pt/KBeta-TEA.

3.2 Catalytic performance

3.2.1 Comparison of Pt/KBeta-SDS with Pt/KBeta-TEA. Fig. 4 shows the dependence of the catalytic activities on the reaction temperature in the catalytic oxidation of toluene over the Pt/KBeta-SDS, Pt/KBeta-TEA, Pt/KBeta-SDS-unreduced and Pt/KBeta-TEA-unreduced catalysts. The conversion of toluene increases rapidly at a certain temperature. It is possible that the actual temperature of the catalytic site is higher than the recorded value as a result of an exothermic reaction. However, it is believed that the temperature at which the conversion is rapidly increased, the ignition temperature, or the temperature at which there is almost full conversion, may be a measure of the catalytic activity. Therefore T_5, T_{50} and T_{98} are used to compare the activities of the catalysts (Table 3). The activities of the reduced catalysts are higher than those of the unreduced catalysts and are positively related to the proportion of Pt^0 species in the catalysts, as observed from the XPS results (Table 2). These results suggest that the Pt^0 species may be the active centres for the conversion of toluene into CO_2 and H_2O.[24,30,31]

It was also found that Pt/KBeta-SDS was more active than Pt/KBeta-TEA. For example, Pt/KBeta-SDS gives a T_{98} for toluene as low as 150 °C, which is lower than that of Pt/KBeta-TEA (160 °C; Table 3). This may be interpreted as a result of the difference in the content of K^+ and terminal silanol defects.[33–36] A higher K^+ content should result in both the formation of more Pt^0 species and a stronger adsorption of toluene in the catalysts (Table 2, Fig. 3); fewer terminal silanol defects favour the stronger adsorption of toluene[33,36] (Fig. 3), which is helpful for the activation of toluene for conversion to CO_2 and H_2O.

3.2.2 Activities of Pt/KBeta-SDS under various conditions. Fig. 5 shows the activities of Pt/KBeta-SDS in the catalytic oxidation of toluene under feed gases with various RH and CO_2 concentrations; the T_5, T_{50} and T_{98} values are presented in Table 4. The activity of the Pt/KBeta-SDS catalyst reduces slightly when the RH of the feed gases is 50%, indicating that there is an inhibition effect of H_2O as a result of the competitive adsorption of H_2O in the oxidation reaction.[31,50] However, the presence of

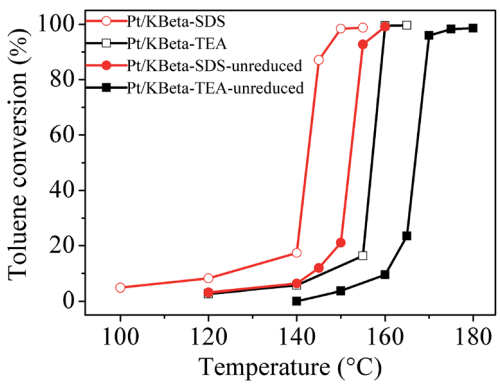

Fig. 4 Catalytic oxidation of toluene over the Pt/KBeta-SDS, Pt/KBeta-TEA, Pt/KBeta-SDS-unreduced and Pt/KBeta-TEA-unreduced catalysts.

Table 3 Catalytic data for toluene oxidation over the Pt/KBeta-SDS and Pt/KBeta-TEA catalysts

	Activity (°C)		
Catalyst	T_5	T_{50}	T_{98}
Pt/KBeta-SDS	101	142	150
Pt/KBeta-TEA	135	157	160
Pt/KBeta-SDS-unreduced	132	152	159
Pt/KBeta-TEA-unreduced	152	167	175

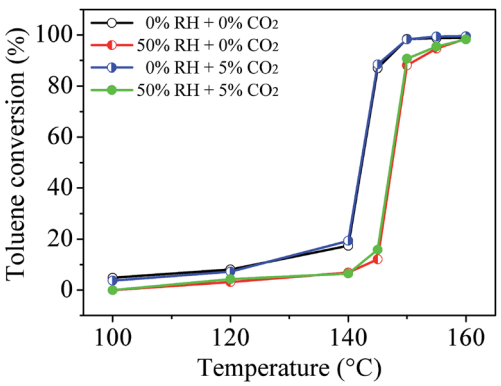

Fig. 5 Catalytic oxidation of toluene over the Pt/KBeta-SDS catalyst under feed gases with various RH and CO_2 concentrations.

Table 4 Catalytic data for toluene oxidation over the Pt/KBeta-SDS catalyst under feed gases with various RH and CO_2 concentrations

		Activity (°C)		
RH[a] (%)	CO_2 concentration (%)	T_5	T_{50}	T_{98}
0	0	101	142	150
50	0	130	147	160
0	5	107	142	150
50	5	126	147	160

[a] Relative humidity.

5% CO_2 in the feed gases did not influence the catalytic activity, indicating that there was no inhibition effect from CO_2. Even in the presence of both H_2O and CO_2, only the inhibition effect of H_2O was observed, indicating that there was no synergistic inhibition effect of H_2O and CO_2.

Fig. 6 shows the dependence of the catalytic activities on reaction time in the catalytic oxidation of toluene over Pt/KBeta-SDS at 150 and 160 °C in the absence or presence of CO_2 and H_2O. Neither CO nor small organic molecules could be detected in the tail gases; CO_2 and H_2O were the only products observed. When the reaction temperature was 150 °C, the activity was very stable during 20 h tests (Fig. 6a). There was no loss of activity after the addition of CO_2. However, the addition of H_2O leads to an obvious reduction in the conversion of toluene (Fig. 6b). The toluene conversion could be completely recovered by stopping the addition of H_2O in the feed gases, indicating that the

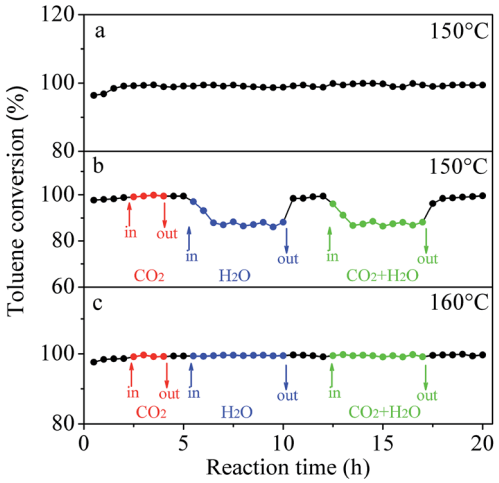

Fig. 6 Dependence of activities on reaction time in the catalytic oxidation of toluene over Pt/KBeta-SDS at temperatures of (a) 150, (b) 150 and (c) 160 °C in the absence or presence of CO_2 (5%) and H_2O (50% RH).

inhibition effect of H_2O is reversible. When the reaction temperature was increased to 160 °C, there was no significant decrease in the conversion of toluene during 20 h tests, even in the presence of CO_2 and H_2O (Fig. 6c). These results indicate that the inhibition effect of H_2O could be completely avoided at 160 °C.

Fig. 7 shows the effect of the SV on activity in the catalytic oxidation of toluene over Pt/KBeta-SDS; the T_5, T_{50} and T_{98} values are presented in Table 5. When the SV was 30 000 mL g^{-1} h^{-1}, the T_5, T_{50} and T_{98} values of the catalyst were 86, 142 and 148 °C, respectively. When the SV reached 60 000 mL g^{-1} h^{-1}, the T_5, T_{50}, and T_{98} values were 101, 142, and 150 °C, respectively. Increasing the SV to 120 000 mL g^{-1} h^{-1}, the T_5, T_{50} and T_{98} values were 111, 143 and 155 °C, respectively. These values are much lower than those reported previously[8,9,23,51,52] (Table 5). These results show that Pt/KBeta-SDS is an active catalyst for the catalytic removal of VOCs.

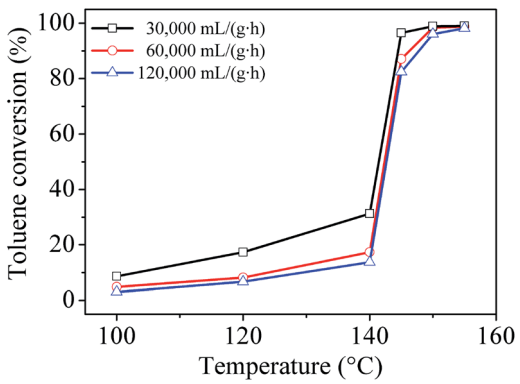

Fig. 7 Catalytic oxidation of toluene over Pt/KBeta-SDS under various SV values.

Table 5 Catalytic data for oxidation of toluene over various catalysts

Catalyst	SV[a] [mL g^{-1} h^{-1}]	$C_{toluene}$[b] (ppm)	Activity (°C)			Ref.
			T_5	T_{50}	T_{98}	
Pt/KBeta-SDS	30 000	1000	86	142	148	This work
	60 000		101	142	150	
	120 000		111	143	155	
$Mn_{0.5}Ce_{0.5}$	50 000	600			260	51
$LaMnO_3$	40 000	1000			265	8
1% Pt/Al_2O_3	153 000	225			260	52
Pd–Au/TiO_2	60 000	1000			230	23
6.4% Au/$LaSrMnO_3$	20 000	1000			180	9

[a] Space velocity. [b] Concentration of toluene.

4. Conclusions

The K^+ form of an aluminium-rich Beta-supported Pt nanoparticle catalyst (Pt/KBeta-SDS) was successfully prepared and tested for the catalytic removal of 1000 ppm toluene. The results show that the Pt/KBeta-SDS catalyst is very active, giving a T_{98} value as low as 150 °C. The superior activity was positively related to the Pt/KBeta-SDS with a high content of Pt^0 species and strong toluene adsorption, which may be reasonably attributed to the abundant K^+ species and the few terminal silanol defects of KBeta-SDS. More importantly, the addition of CO_2 and H_2O in the feed gases does not influence the activities of the Pt/KBeta-SDS catalyst when the reaction temperature is >160 °C. This feature is potentially important in future practical applications of this catalyst.

Acknowledgements

This work was supported by the National Natural Science Foundation of China (21422306, 21273197 and 21203165) and the National High-Tech Research and Development Program of China (2013AA065301).

Notes and references

1 J. J. Spivey, *Ind. Eng. Chem. Res.*, 1987, **26**, 2165.
2 L. F. Liotta, *Appl. Catal., B*, 2010, **100**, 403.
3 T. Barakat, J. C. Rooke, H. L. Tidahy, M. Hosseini, R. Cousin, J.-F. Lamonier, J.-M. Giraudon, G. De Weireld, B.-L. Su and S. Siffert, *ChemSusChem*, 2011, **4**, 1420.
4 W. B. Li, J. X. Wang and H. Gong, *Catal. Today*, 2009, **148**, 81.
5 C. B. Zhang, H. He and K. Tanaka, *Appl. Catal., B*, 2006, **65**, 37.
6 C. B. Zhang, F. D. Liu, Y. P. Zhai, H. Ariga, N. Yi, Y. C. Liu, K. Asakura, M. Flytzani-Stephanopoulos and H. He, *Angew. Chem., Int. Ed.*, 2012, **51**, 9628.
7 J.-H. Park, B. Kim, C.-H. Shin, G. Seo, S. H. Kim and S. B. Hong, *Top. Catal.*, 2009, **52**, 27.
8 Y. X. Liu, H. X. Dai, Y. C. Du, J. G. Deng, L. Zhang, Z. X. Zhao and C. T. Au, *J. Catal.*, 2012, **287**, 149.
9 Y. X. Liu, H. X. Dai, J. G. Deng, X. W. Li, Y. Wang, H. Arandiyan, S. H. Xie, H. G. Yang and G. S. Guo, *J. Catal.*, 2013, **305**, 146.
10 C. He, J. J. Li, P. Li, J. Cheng, Z. P. Hao and Z.-P. Xu, *Appl. Catal., B*, 2010, **96**, 466.
11 C. He, F. W. Zhang, L. Yue, X. S. Shang, J. S. Chen and Z. P. Hao, *Appl. Catal., B*, 2012, **111**, 46.
12 Z. Z. Zhu, G. Z. Lu, Z. G. Zhang, Y. Guo, Y. L. Guo and Y. Q. Wang, *ACS Catal.*, 2013, **3**, 1154.
13 H. Huang, Q. G. Dai and X. Y. Wang, *Appl. Catal., B*, 2014, **158**, 96.
14 D. Y. C. Leung, X. L. Fu, D. Q. Ye and H. B. Huang, *Kinet. Catal.*, 2012, **53**, 239.
15 A. M. Harling, D. J. Glover, J. C. Whitehead and K. Zhang, *Environ. Sci. Technol.*, 2008, **42**, 4546.
16 H. C. Genuino, S. Dharmarathna, E. C. Njagi, M. C. Mei and S. L. Suib, *J. Phys. Chem. C*, 2012, **116**, 12066.
17 Q. G. Huang, S. F. Zuo and R. X. Zhou, *Appl. Catal., B*, 2010, **95**, 327.
18 B. de Rivas, R. Lopez-Fonseca, C. Jimenez-Gonzalez and J. I. Gutierrez-Ortiz, *J. Catal.*, 2011, **281**, 88.
19 L. Becker and H. Forster, *J. Catal.*, 1997, **170**, 200.
20 L. Becker and H. Forster, *Appl. Catal., B*, 1998, **17**, 43.
21 H. L. Tidahy, S. Siffert, J.-F. Lamonier, R. Cousin, E. A. Zhilinskaya, A. Aboukais, B.-L. Su, X. Canet, G. De Weireld, M. Frere, J.-M. Giraudon and G. Leclercq, *Appl. Catal., B*, 2007, **70**, 377.
22 H. L. Tidahy, M. Hosseni, S. Siffert, R. Cousin, J.-F. Lamonier, A. Aboukais, B.-L. Su, J.-M. Giraudon and G. Leclercq, *Catal. Today*, 2008, **137**, 335.
23 M. Hosseini, T. Barakat, R. Cousin, A. Aboukais, B.-L. Su, G. De Weireld and S. Siffert, *Appl. Catal., B*, 2012, **111**, 218.
24 J. Tsou, L. Pinard, P. Magnoux, J. L. Figueiredo and M. Guisnet, *Appl. Catal., B*, 2003, **46**, 371.
25 J. Tsou, P. Magnoux, M. Guisnet, J. J. M. Orfao and J. L. Figueiredo, *Appl. Catal., B*, 2004, **51**, 129.
26 J. Tsou, P. Magnoux, M. Guisnet, J. J. M. Orfao and J. L. Figueiredo, *Appl. Catal., B*, 2005, **57**, 117.
27 L. Pinard, J. Mijoin, P. Ayrault, C. Canaff and P. Magnoux, *Appl. Catal., B*, 2004, **51**, 1.

28 R. Beauchet, J. Mijoin and P. Magnoux, *Appl. Catal., B*, 2009, **88**, 106.
29 L. M. Gandia, A. Gil and S. A. Korili, *Appl. Catal., B*, 2001, **33**, 1.
30 C. Y. Chen, J. Zhu, F. Chen, X. J. Meng, X. M. Zheng, X. H. Gao and F.-S. Xiao, *Appl. Catal., B*, 2013, **140**, 199.
31 C. Y. Chen, X. Wang, J. Zhang, S. X. Pan, C. Q. Bian, L. Wang, F. Chen, X. J. Meng, X. M. Zheng, X. H. Gao and F.-S. Xiao, *Catal. Lett.*, 2014, **144**, 1851.
32 F. J. Liu, S. F. Zuo, C. Wang, J. T. Li, F.-S. Xiao and C. Z. Qi, *Appl. Catal., B*, 2014, **148**, 106.
33 X. J. Meng and F.-S. Xiao, *Chem. Rev.*, 2014, **114**, 1522.
34 B. Xie, J. W. Song, L. M. Ren, Y. Y. Ji, J. X. Li and F.-S. Xiao, *Chem. Mater.*, 2008, **20**, 4533.
35 B. Xie, H. Y. Zhang, C. G. Yang, S. Y. Liu, L. M. Ren, L. Zhang, X. J. Meng, B. Yilmaz, U. Muller and F.-S. Xiao, *Chem. Commun.*, 2011, **47**, 3945.
36 H. Y. Zhang, B. Xie, X. J. Meng, U. Muller, B. Yilmaz, M. Feyen, S. Maurer, H. Gies, T. Tatsumi, X. H. Bao, W. P. Zhang, D. De Vos and F.-S. Xiao, *Microporous Mesoporous Mater.*, 2013, **180**, 123.
37 Y. Wang, J. W. Ren, K. Deng, L. L. Gui and Y. Q. Tang, *Chem. Mater.*, 2000, **12**, 1622.
38 N. H. An, S. Y. Li, P. N. Duchesne, P. Wu, W. L. Zhang, J. F. Lee, S. Cheng, P. Zhang, M. J. Jia and W. X. Zhang, *J. Phys. Chem. C*, 2013, **117**, 21254.
39 H. Song, R. M. Rioux, J. D. Hoefelmeyer, R. Komor, K. Niesz, M. Grass, P. D. Yang and G. A. Somorjai, *J. Am. Chem. Soc.*, 2006, **128**, 3027.
40 T. Teranishi, M. Hosoe, T. Tanaka and M. Miyake, *J. Phys. Chem. B*, 1999, **103**, 3818.
41 G. X. Chen, Y. Zhao, G. Fu, P. N. Duchesne, L. Gu, Y. P. Zheng, X. F. Weng, M. S. Chen, P. Zhang, C.-W. Pao, J.-F. Lee and N. F. Zheng, *Science*, 2014, **344**, 495.
42 Q. Fu, W.-X. Li, Y. X. Yao, H. Y. Liu, H.-Y. Su, D. Ma, X.-K. Gu, L. M. Chen, Z. Wang, H. Zhang, B. Wang and X. H. Bao, *Science*, 2010, **328**, 1141.
43 P. Treesukol, K. Srisuk, J. Limtrakul and T. N. Truong, *J. Phys. Chem. B*, 2005, **109**, 11940.
44 D. C. Koningsberger and B. C. Gates, *Catal. Lett.*, 1992, **14**, 271.
45 B. L. Mojet, J. T. Miller, D. E. Ramaker and D. C. Koningsberger, *J. Catal.*, 1999, **186**, 373.
46 D. E. Ramaker, J. de Graaf, J. A. R. van Veen and D. C. Koningsberger, *J. Catal.*, 2001, **203**, 7.
47 S. Siffert, J.-L. Schmitt, J. Sommer and F. Garin, *J. Catal.*, 1999, **184**, 19.
48 R. Yoshimoto, K. Hara, K. Okumura, N. Katada and M. Niwa, *J. Phys. Chem. C*, 2007, **111**, 1474.
49 R. Yoshimoto, T. Ninomiya, K. Okumura and M. Niwa, *Appl. Catal., B*, 2007, **75**, 175.
50 L. J. Xie, F. D. Liu, L. M. Ren, X. Y. Shi, F.-S. Xiao and H. He, *Environ. Sci. Technol.*, 2014, **48**, 566.
51 D. Delimaris and T. Ioannides, *Appl. Catal., B*, 2008, **84**, 303.
52 M. Paulis, H. Peyrard and M. Montes, *J. Catal.*, 2001, **199**, 30.

